Sensors and Actuators: A. Physical 332 (2021) 113173

Contents lists available at ScienceDirect

Sensors and Actuators: A. Physical

journal homepage: www.elsevier.com/locate/sna

# A polymer based self-powered ethanol gas sensor to eliminate the interference of ultraviolet light

Mingmin Hao, Ruichao Zhang, Xiaofeng Jia, Xiang Gao, Weihao Gao, Li Cheng*, Yong Qin*

*Institute of Nanoscience and Nanotechnology, School of Materials and Energy, Lanzhou University, Gansu 730000, PR China*

ARTICLE INFO

*Article history:*
Received 12 July 2021
Received in revised form 22 September 2021
Accepted 8 October 2021
Available online 11 October 2021

*Keywords:*
Gas sensor
Triboelectric nanogenerator
Self-powered sensor
Stability

ABSTRACT

As a kind of gas sensors, self-powered gas sensor shows significant advantages in large-scale applications such as the internet of things. On the other hand, triboelectric nanogenerator is an ideal power source to fabricate self-powered gas sensor for its high power output and wide variety of driving source. More importantly, it is indispensable to eliminate the influence of environmental factors considering the practical application of gas sensors. In this work, by utilizing the polymer materials with wide bandgap, a polymer based self-powered ethanol gas sensor (PB-SPES) is designed to eliminate the influence of ultraviolet (UV) light in the environment and detect the ethanol gas reliably. Compared with a zinc oxide (ZnO) based self-powered ethanol gas sensor, the PB-SPES shows good stability under UV light illumination.



## 1. Introduction

Gas sensing is an important technology that is widely used in our daily life, including the detection of toxic analytes and explosive gas, monitoring of environment pollution and air quality [1–4]. Among these applications, a large number of gas sensors are likely needed to work in large area, which makes their powering quite challenging [5], since powering these devices with wires is costly and easy to be damaged. Besides, the use of traditional batteries needs to be replaced regularly, which is inconvenient in many situations. Thus, it is necessary to develop self-powered gas sensors to harvest energy from the environment, and convert it into electric power to supply the energy cost of themselves [6,7]. Compared with conventional gas sensors, these self-powered ones exhibit the approximate performance with much smaller power consumption. Besides, the size of self-powered sensor is drastically reduced, where the power supply unit is no longer needed [8].

As a device collecting mechanical energy in the environment, triboelectric nanogenerator (TENG) is an ideal power source for self-powered gas sensors. There are mainly two routes to fabricate a TENG based self-powered gas sensor [9]. One is to connect the TENG to a conventional gas sensor, where the voltage across the two electrodes of the gas sensor or the current flowing through the gas sensor varies with gas concentrations [10]. The other is to directly use a material sensitive to gas as the friction layer of the TENG, where the output voltage or current of the TENG varies with gas concentrations [11]. The second route shows significant advantages for its simple construction and easy fabrication. Semiconductor materials, whose conductivity can vary in different gases due to the charge transfer between the material and gas molecules, are usually used in fabricating gas sensors. Therefore, using semiconductor materials such as zinc oxide (ZnO), polyaniline or indium tin oxide (ITO) as friction layers, a series of TENGs have been developed for self-powered gas detecting such as hydrogen ($H_2$), ammonia ($NH_3$), ethanol gas and so on [12–14].

However, owing to the generation of electron-hole pairs when excited by photons with energy higher than the bandgap of semiconductor materials, TENGs based on semiconductor materials as the friction layer will also respond to the light especially the ultraviolet (UV) light in the environment. For example, TENG using ZnO nanowires (NWs) as a friction layer exhibits intense response to UV light, where a decrease of 10% in output current is observed when exposed to UV light with the intensity of 780 pW/cm$^2$ [15]. Thus, in practical applications of these devices, it is very difficult to eliminate the influence of UV light in the environment.

To solve this problem, using insulator materials instead of the semiconductor materials as the friction layer can be a feasible way. Bandgaps of insulator materials are larger than that of semiconductor materials, and the absorption of photons will not generate electron-hole pairs in these materials. Hence, it is possible to eliminate the influence of UV light through using only insulator materials as the friction layers. In this work, polyimide (PI) NW array and porous polyamide (PA) film are designed as the friction layers respectively, and a polymer based self-powered ethanol gas sensor (PB-SPES) are fabricated. Benefiting from the high specific surface area of the PI NW array,

* Corresponding authors.
*E-mail addresses:* chengl2007@live.cn (L. Cheng), qinyong@lzu.edu.cn (Y. Qin).

https://doi.org/10.1016/j.sna.2021.113173
0924-4247/

the PB-SPES shows good sensitivity to ethanol gas with the concentration ranging from 500 to 10,000 ppm. Furthermore, the PB-SPES shows good stability under the interference of UV light illumination compared to semiconductor material based self-powered gas sensor. The device also possesses good selectivity and repeatability, which facilitates its promising application.

## 2. Materials and methods

### 2.1. Fabrication of the PI NW array

A piece of clean PI film is placed on the electrode of the RIE machine. After vacuum to $3 \times 10^{-3}$ Pa, the film is etched at 2 Pa pressure, 100 W input power and 400 V automatic bias with 60 standard cubic centimeters per minute (sccm) oxygen gas flow for 60 min. This film is subsequently immersed in 2 M hydrochloric acid solution for 30 min to remove the metal or metal oxide particles existing on the surface of NWs and then wash with deionized water. After drying in an oven at 80 °C for 30 min, PI NW array is fabricated on one surface of the PI film.

### 2.2. Preparation of the PA solution

2 g PA is mixed with 16 g formic acid in a 50 mL triangular flask [16], then it is stirred for 1 h to ensure the dissolution of PA. Afterwards, the PA solution is prepared successfully.

### 2.3. Fabrication of the PB-SPES

PI NW array is first prepared on a piece of 100 μm thick PI film (4 cm × 4 cm in size) and then Ag electrode (3 cm × 3 cm in size) is sputtered on the other side of the film to fabricate one part of the device. On the other piece of 100 μm thick PI film (4 cm × 4 cm in size), Ag electrode (3 cm × 3 cm in size) is first sputtered on one side of the film and the PA porous film is spin-coated on another side with the speed of 1500 rpm for 60 s and drying naturally to fabricate the other part of the device. The PB-SPES is fabricated after connecting copper wires on the Ag electrodes.

### 2.4. Synthesis of the ZnO NWs

The ZnO NWs are synthesized in a quartz tube furnace using ZnO and graphite powder as the source material, oxygen gas as the reaction gas, and argon gas as the carrier gas. 3.2558 g ZnO powder and 0.4807 g graphite powder are grinded in an agate mortar to make the powder mix uniformly. Then, the mixed powder is placed in an alumina boat at the middle of the tube furnace, and the substrate is put 12 cm away from the alumina boat in the furnace. 100 sccm argon gas and 10 sccm oxygen gas is introduced into the quartz tube and the tube is pumped to 190 Pa. Then the furnace is heated to 950 °C in 19 min and maintained at this temperature for 30 min. ZnO NWs are grown on the substrate after the furnace is cooled down to room temperature.

### 2.5. Fabrication of the TENG with ZnO NWs

The ZnO NWs is first synthesized on the surface of a piece of quartz glass with ITO electrode as one part of the device, and PI film with porous PA film and Ag electrodes respectively on its two sides as the other part of the device. The TENG with ZnO NWs are fabricated after connecting copper wires on the electrodes.

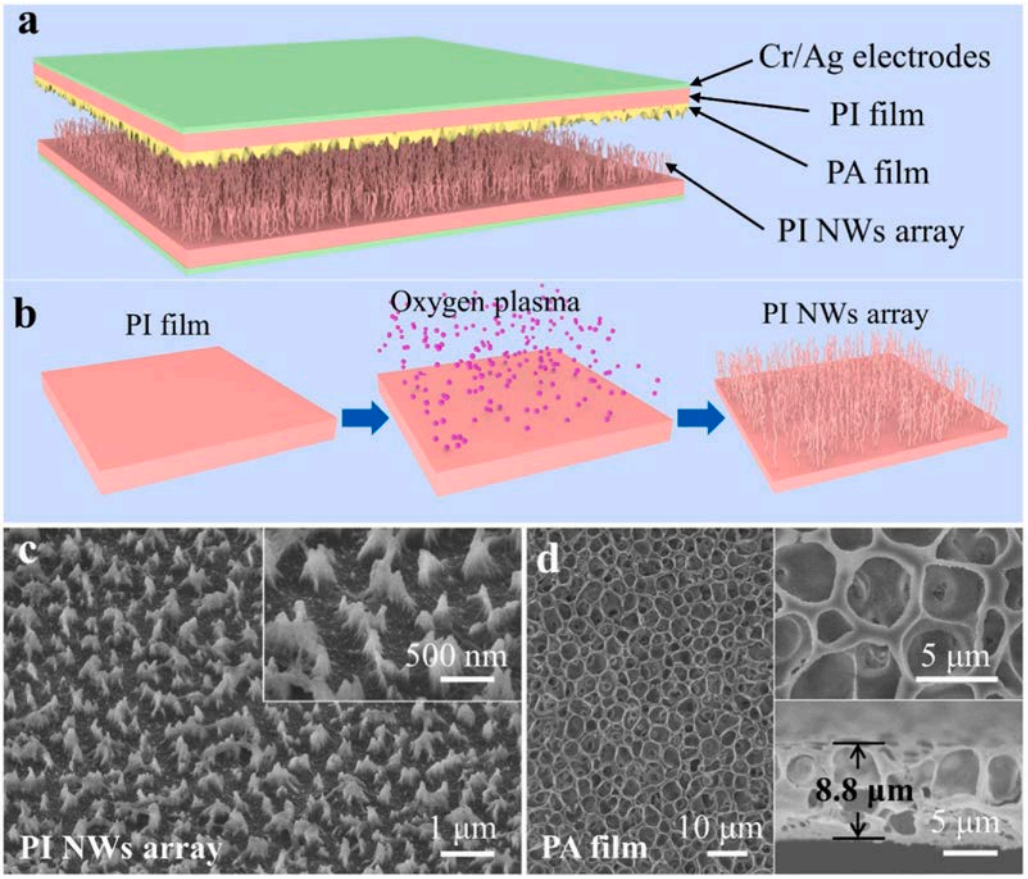


**Fig. 1.** Structure and fabrication of the PB-SPES. (a) Schematic diagram of the PB-SPES. (b) Fabrication process of the PI NW array. (c) 30º oblique view SEM image of the PI NW array, the insert shows the enlarged SEM images of the PI NWs array. (d) SEM image of the porous PA film, the inserts show the enlarged SEM image of the PA film and the sectional view SEM image of the PA film.

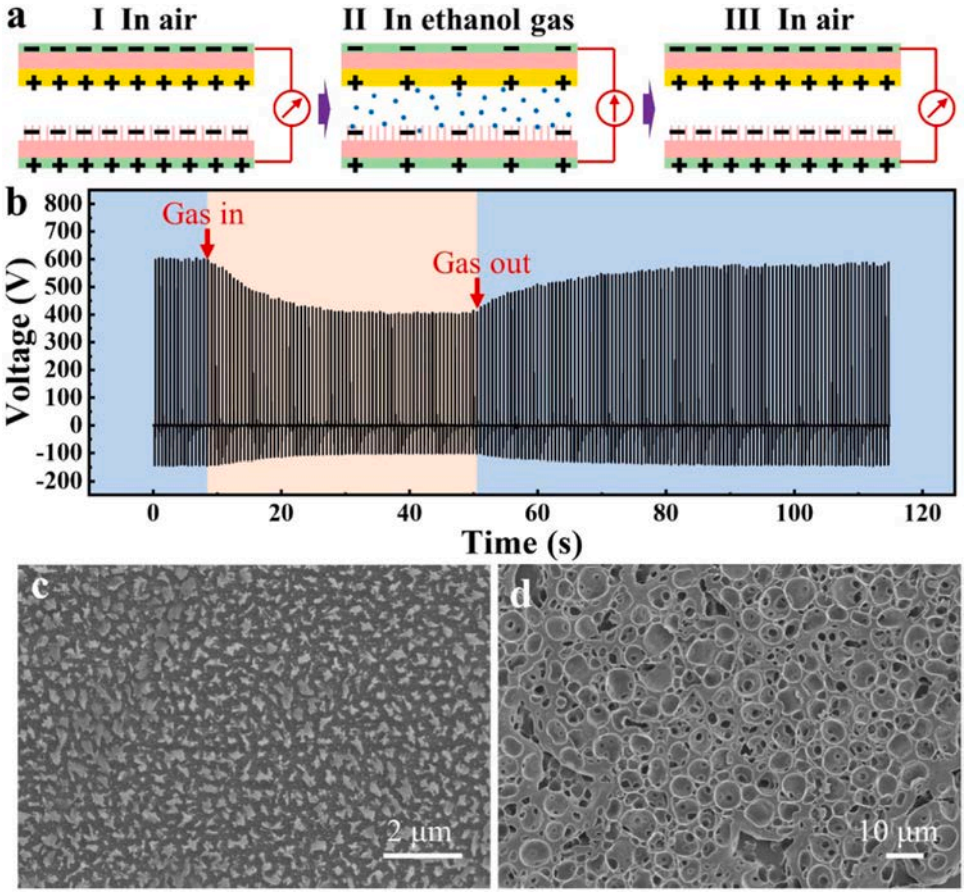


**Fig. 2.** Working process of the PB-SPES. (a) Schematic diagram of the working mechanism of the PB-SPES, (I) to (III) respective show distribution of charges on the PB-SPES at the stage of in air, in air with ethanol gas and back in air. (b) Variation of PB-SPES's output voltage in pure air and 10,000 ppm ethanol gas. (c) and (d) SEM images of PI NWs (c) and PA film (d) after the PB-SPES working and exposing to ethanol gas.

### *2.6. Measurement of the PB-SPES and the ZnO-SPES*

The devices are measured with a current amplifier (SR570, Stanford Research Systems, USA) and a data acquisition card (BNC-2120, National Instruments, USA).

## 3. Results and discussions

As Fig. 1a shows, the PB-SPES contains two pieces of 4 cm × 4 cm PI films with the thickness of 100 μm. PI NW array and porous PA film are respectively fabricated onto one side of each film as the friction layers to generate charges *via* the working process. Then, Cr/Ag electrodes with the size of 3 cm × 3 cm are fabricated onto the back side of each film to collect and transport electrical energy to the circuit. The PI NW array is fabricated *via* reactive ion etching (RIE) (shown in Fig. 1b) and the porous PA film is fabricated *via* spin-coating. As shown in the scanning electron microscope (SEM) images of Fig. 1c, the diameter and length of the PI NWs are about 200 nm and 700 nm respectively, and the NWs are distributed as islands on the surface of PI film. Fig. 1d shows, micropores with the diameter of about 5 μm uniformly

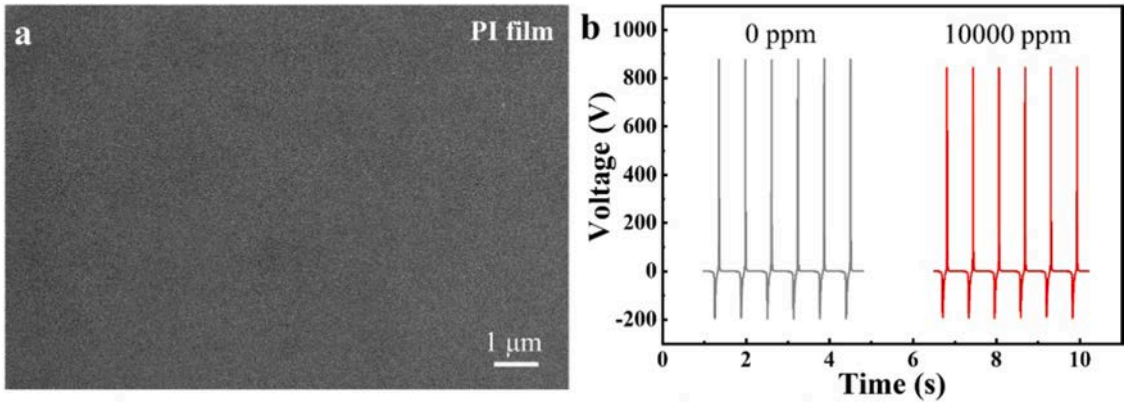


**Fig. 3.** Effect of the nanostructure on the response of the PB-SPES. (a) SEM image of the smooth PI film. (b) The output voltage of a TENG using smooth PI film in air and in 10,000 ppm ethanol gas.

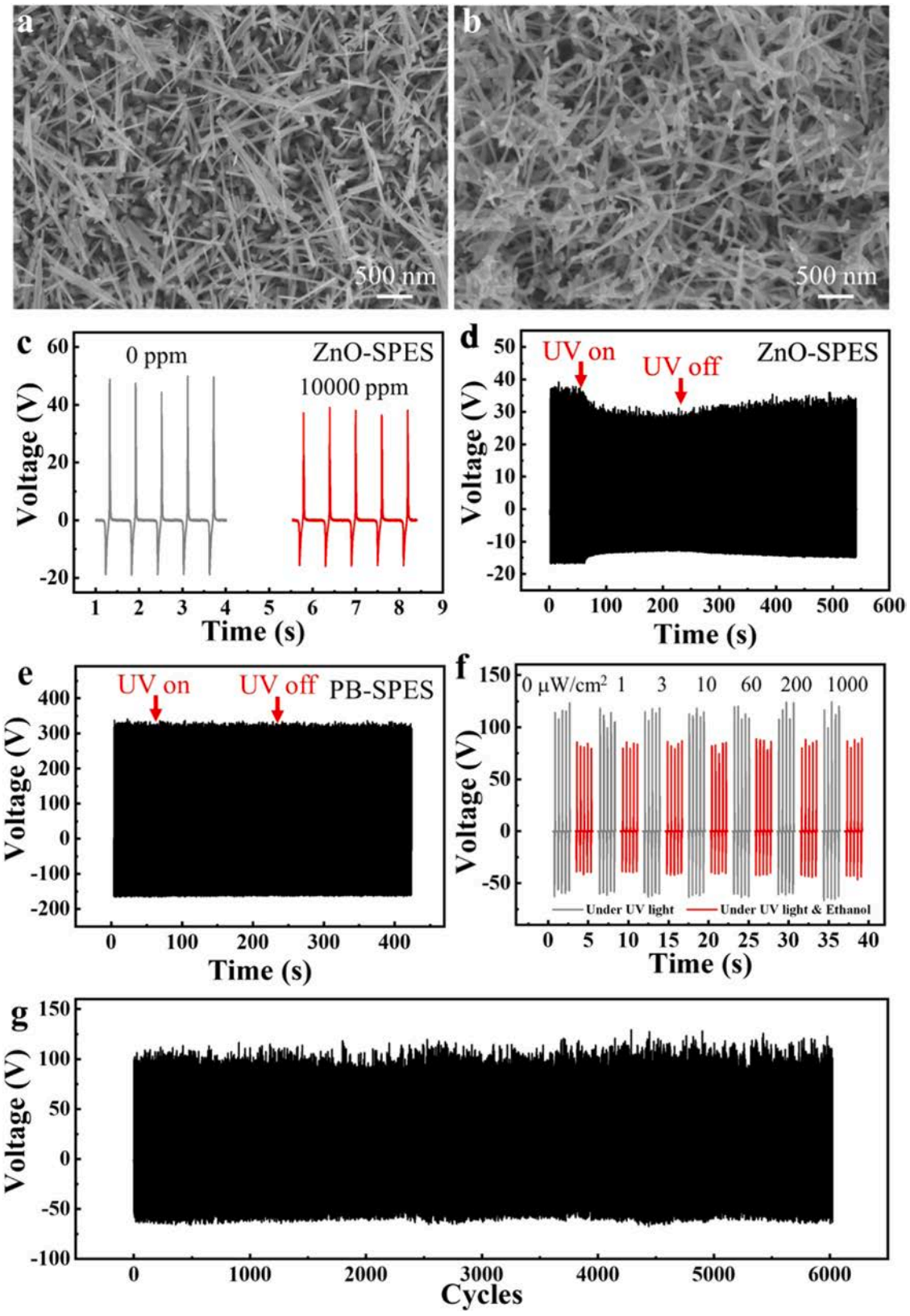


**Fig. 4.** Stability of the PB-SPES in UV light. (a) SEM image of ZnO NWs. (b) SEM image of ZnO NWs after the PB-SPES working and exposing to ethanol gas. (c) The output voltage of a TENG using ZnO NWs and PA porous film as friction layers in air and 10,000 ppm ethanol gas. (d) Variation of the output voltage of the TENG using ZnO NWs and PA porous film as friction layers under 1 mW/cm$^2$ UV light. (e) Variation of the output voltage of the PB-SPES under 1 mW/cm$^2$ UV light. (f) The output voltage of PB-SPES under 1, 3, 10, 60, 200, 1000 μW/m$^2$ UV light intensity with (red lines) and without (grey lines) 10,000 ppm ethanol gas. (g) The output voltage of PB-SPES with exposer of ethanol as well as with 1 mW/cm$^2$ UV illumination for about 6000 cycles.

distribute on the surface of the PA film and the thickness of the PA film is about 8.8 μm. The micro/nano structures existing on the friction layers contributes to the enhancement of TENG's performance [17]. Details of the fabrication process of the PB-SPES and the friction layers are given in the Materials and methods.

The working mechanism of the PB-SPES is shown in Fig. 2a. As Fig. 2aI shows, when the PB-SPES works in air, the PI NW array rubs with the porous PA film and attract electrons from the PA film [18]. As a result, the negative charge is generated on the PI NW array, while the positive charge is generated on the PA film after rubbing, and the free charge flows through the external circuit to balance the potential difference. As Fig. 2aII shows, when the PB-SPES contacts with ethanol gas, ethanol molecules are adsorbed on the friction layers. Primitively, there are many oxygen atoms existing in the molecular structure of PI in the atmospheric environment, which plays an important role in attracting the electrons from the PA film. After the ethanol molecules are adsorbed on the PI NWs, more hydrogen atoms are exposed on the surface, which will obviously decrease the ability to attract electrons from PA film. As a result, both the positive and negative charges existing on the friction layer decrease, which leads to an output decrease of PB-SPES. When the PB-SPES works in atmospheric environment again (shown in Fig. 2aIII), due to the desorption of ethanol molecules, the ability of PI NWs attracting electrons recovers. In a word, owing to the adsorption of ethanol molecules on the PI NWs, the output of the PB-SPES will decrease in ethanol gas and recovery in air.

Changes of the output voltage of the PB-SPES in ethanol gas are then measured to verify the working mechanism and gas sensitivity of the device. As the result shown in Fig. 2b, after contacting with 10,000 ppm ethanol gas, the output voltage of the PB-SPES decreases intensively from 600 V to 400 V in about 28 s. And after venting the ethanol gas, the output voltage of PB-SPES recovers in about 60s Fig. 2c and d respectively show the SEM images of PI NWs and PA film after working and exposing to ethanol gas. We can see that the morphology of PI NWs and PA film does not change except for the slanting of a few PI NWs, which affect little to the performance of the PB-SPES. The experimental result confirms with the working mechanism of the PB-SPES and demonstrates the ability of the PB-SPES as an ethanol gas sensor.

According to the working mechanism of the PB-SPES, adsorption of ethanol molecules on the frictional layers should be a key point of its response to ethanol gas. As we all know, specific surface area of materials is one important parameter which will significantly influence the adsorption of gas molecules on their surfaces. Specifically, a material with larger specific surface area provide more sites to interact with gas molecules [19]. It has been reported that fabricating nanostructure on the surface of friction layer is greatly beneficial to the increase of specific surface area as well as the output [20]. Thus, it could be easily inferred that the nanostructures on the frictional layer will enhance the chance of ethanol molecules adsorbed on its surface and further improve the sensitivity of PB-SPES to ethanol gas. In order to verify the ability of the nanostructures to improve the performance of the PB-SPES, another TENG is fabricated and measured, where the PI NW array is replaced with a smooth PI film. Fig. 3a shows the SEM image of the smooth PI film. As Fig. 3b shows, the output voltage of the TENG with smooth PI film only decreases by about 3.8% to 10,000 ppm ethanol gas compared with that in air, which is about one-tenth of the PB-SPES's response under the same ethanol gas concentration. This result indicates that nanostructures on the surface of the friction layer contributes greatly to improve the sensitivity of PB-SPES to ethanol gas.

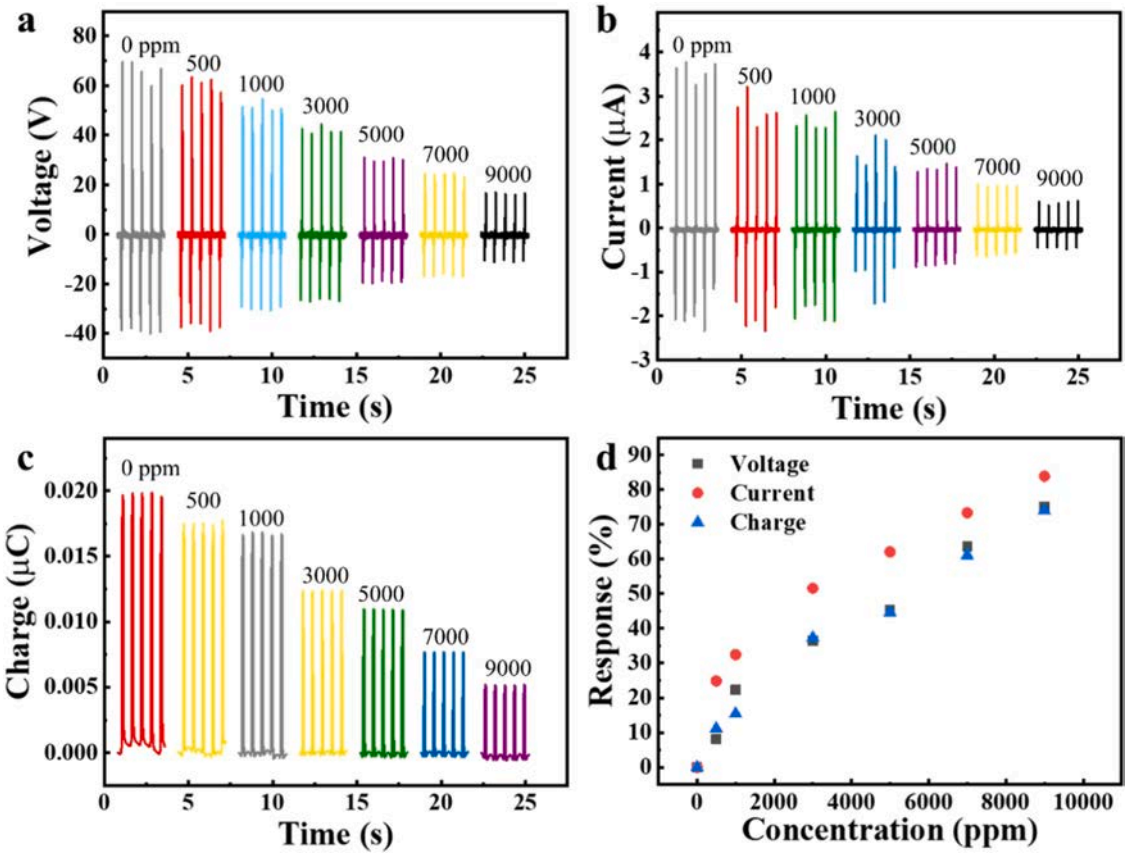


**Fig. 5.** The output of the PB-SPES changes with ethanol gas concentration. (a) to (c) respectively show the output voltage, current and transferred charge of one peak of the PB-SPES at ethanol gas concentrations of 0, 500, 1000, 3000, 5000, 7000 and 9000 ppm. (d) Response of PB-SPES *versus* varying concentrations of ethanol gas.

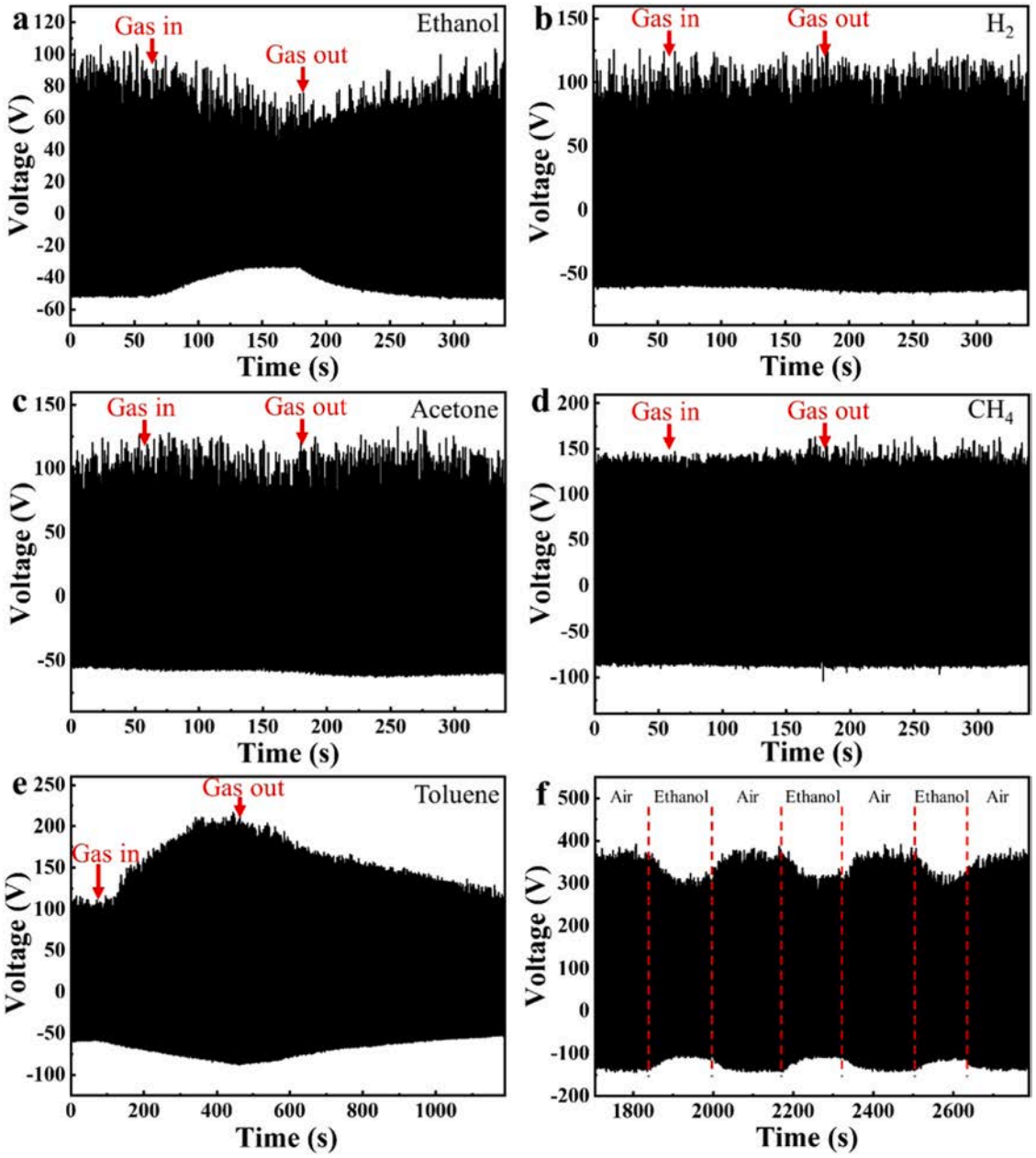


**Fig. 6.** Selectivity and repeatability of the PB-SPES. (a) to (e) respectively show the output voltage of the PB-SPES under 0 and 10,000 ppm ethanol gas, $H_2$, acetone gas, $CH_4$ and toluene gas. (f) Three response/recovery cycles of the PB-SPES under 0 and 10,000 ppm ethanol gas.

In general, working mechanism of the PB-SPES could be described as follows: 1. As a TENG, the PB-SPES generates electrical signals on the basis of triboelectric effect and electrostatic induction; 2. Ethanol molecules adsorbed on the PI NW array change the atoms exposed on the surface and further lower the electron affinity of PI, hence, the output of the PB-SPES decreases in ethanol gas; 3. Nanostructures on the PI NW array result in very high specific surface area, which benefits the adsorption of ethanol molecules and the sensitivity of the PB-SPES.

Subsequently, we study the ability of the PB-SPES to eliminate the influence of UV light in the environment. In the experiment, we fabricate a ZnO based self-powered ethanol gas sensor (ZnO-SPES) and measure the influence of UV light to the output voltages of the ZnO-SPES and the PB-SPES, respectively. The ZnO-SPES consists of ZnO NWs (SEM image before and after working and exposing to ethanol gas are shown in Fig. 4a and b, respectively) and porous PA film as friction layers. As Fig. 4c shows, compared with its output voltage in air, the output voltage of the TENG with ZnO NWs decreases by 21% in 10,000 ppm ethanol gas, indicating this device could be used for self-powered ethanol gas detection. Then, the PB-SPES and the ZnO-SPES are illuminated with 1 $mW/cm^2$ UV light respectively to measure their stability in UV light. As shown in Fig. 4d, when the ZnO-SPES is illuminated with 1 $mW/cm^2$ UV light, its output voltage also decreases obviously by 22%, which may cause error response in its practical applications. In contrast, as shown in Fig. 4e, the output voltage of PB-SPES remains unchanged when it is illuminated with 1 $mW/cm^2$ UV light. Fig. 4f shows, output of the PB-SPES remain unchanged under different UV light intensity ranging from 1 to 1000 $\mu W/cm^2$, whether in air or in ethanol gas. In order to apply this methodology as large-scale application, we test the PB-SPES with exposer of ethanol as well as with UV illumination for about 6000 cycles and the result shows, output voltage of the PB-SPES remains unchanged (shown in Fig. 4g). This result indicates that the PB-SPES could eliminate the influence of UV light in the

environment through using polymer materials instead of the semiconductor materials which is commonly used in TENG based self-powered gas sensors.

The PB-SPES to different concentrations of ethanol gas as well as its selectivity and repeatability are studied. First, the output voltage and current of PB-SPES in ethanol gas with different concentrations are respectively measured, and the corresponding output charge of one peak is obtained. As shown in Fig. 5a-d, the PB-SPES's output voltage, current and transferred charge all decrease monotonically with the increase of ethanol gas concentration ranging from 500 to 9000 ppm with nearly a linear relationship. To 500 ppm ethanol gas, the PB-SPES exhibits an average reduction of output voltage, current and transferred charge respectively by 8.1%, 24.8% and 11.1%, which is easy to be detected in its practical applications.

Fig. 6a-e show the real-time continuous responding/recovering process of the PB-SPES upon exposure to 10,000 ppm ethanol gas, $H_2$, acetone gas, methane ($CH_4$) and toluene gas. It can be seen that the output voltage of PB-SPES has almost no change after exposing to $H_2$, acetone gas and $CH_4$, and the output voltage of PB-SPES increases after exposing with toluene gas. When ethanol gas is introduced, the output voltage of PB-SPES decreases, which indicates its certain selectivity to ethanol gas. Fig. 6f shows three continuous response/recovery cycles of PB-SPES against 10,000 ppm ethanol gas. In the three cycles, the sensitivity and response/recovery time of the PB-SPES have no significant change of each cycle, which shows that the device has good repeatability. The above-mentioned results prove that the adsorption and desorption of ethanol molecules can reversibly take place in the response and recovery processes, respectively. The relatively short response/recovery time and good repeatability of PB-SPES can pave the way for its practical application.

## 4. Conclusions

In summary, a PB-SPES for self-powered ethanol gas detection is designed and fabricated. As a self-powered device, the PB-SPES could generate electrical energy under external force. It is sensitive to ethanol gas with a concentration ranging from 500 to 10,000 ppm. The high specific surface area of the PI NW array as a friction layer in the PB-SPES considerably increase the sensitivity of the PB-SPES for it is beneficial to the adsorption of gas molecules. Due to the wide bandgap of polymer materials as the ethanol sensitive materials, the PB-SPES can eliminate the influence response of UV light in the environment. Meanwhile, the PB-SPES shows good repeatability and selectivity. This work provides a promising solution for the self-powered gas sensor to eliminate the influence of factors in the environment.

## CRediT authorship contribution statement

The manuscript was written through contributions of all authors. All authors have given approval to the final version of the manuscript.

## Declaration of Competing Interest

The authors declare that they have no known competing financial interests or personal relationships that could have appeared to influence the work reported in this paper.

## Acknowledgement

We sincerely acknowledge the support from National Nature Science Foundation of China (No. 51702377).

## References

[1] J.D. Fowler, M.J. Allen, V.C. Tung, Y. Yang, R.B. Kaner, B.H. Weiller, Practical chemical sensors from chemically derived graphene, ACS Nano 3 (2) (2009) 301–306.
[2] M.I. Mead, O.A.M. Popoola, G.B. Stewart, P. Landshoff, M. Calleja, M. Hayes, J.J. Baldovi, M.W. McLeod, T.F. Hodgson, J. Dicks, A. Lewis, J. Cohen, R. Baron, J.R. Saffell, R.L. Jones, The use of electrochemical sensors for monitoring urban air quality in low-cost, high-density networks, Atmos. Environ. 70 (2013) 186–203.
[3] S.J. Toal, W.C. Trogler, Polymer sensors for nitroaromatic explosives detection, J. Mater. Chem. 16 (28) (2006) 2871–2883.
[4] G.F. Fine, L.M. Cavanagh, A. Afonja, R. Binions, Metal oxide semi-conductor gas sensors in environmental monitoring, Sensors 10 (6) (2010) 5469–5502.
[5] P. Glynne-Jones, N.M. White, Self-powered systems: a review of energy sources, Sens. Rev. 21 (2) (2001) 91–98.
[6] Z.L. Wang, Self-powered nanosensors and nanosystems, Adv. Mater. 24 (2) (2012) 280–285.
[7] Z.L. Wang, G. Zhu, Y. Yang, S. Wang, C. Pan, Progress in nanogenerators for portable electronics, Mater. Today 15 (12) (2012) 532–543.
[8] Z. Wen, Q. Shen, X. Sun, Nanogenerators for self-powered gas sensing, Nano-Micro Lett. 9 (4) (2017) 45.
[9] V. Nguyen, R. Zhu, R. Yang, Environmental effects on nanogenerators, Nano Energy 14 (2015) 49–61.
[10] Z. Wen, J. Chen, M.-H. Yeh, H. Guo, Z. Li, X. Fan, T. Zhang, L. Zhu, Z.L. Wang, Blow-driven triboelectric nanogenerator as an active alcohol breath analyzer, Nano Energy 16 (2015) 38–46.
[11] H. Zhang, Y. Yang, Y. Su, J. Chen, C. Hu, Z. Wu, Y. Liu, C. Ping Wong, Y. Bando, Z.L. Wang, Triboelectric nanogenerator as self-powered active sensors for detecting liquid/gaseous water/ethanol, Nano Energy 2 (5) (2013) 693–701.
[12] S. Cui, Y. Zheng, T. Zhang, D. Wang, F. Zhou, W. Liu, Self-powered ammonia nanosensor based on the integration of the gas sensor and triboelectric nanogenerator, Nano Energy 49 (2018) 31–39.
[13] S.H. Shin, Y.H. Kwon, Y.H. Kim, J.Y. Jung, J. Nah, Triboelectric hydrogen gas sensor with Pd functionalized surface, Nanomaterials 6 (10) (2016) 186.
[14] A.S.M.I. Uddin, G.-S. Chung, A self-powered active hydrogen gas sensor with fast response at room temperature based on triboelectric effect, Sens. Actuator B-Chem. 231 (2016) 601–608.
[15] L. Cheng, Y. Zheng, Q. Xu, Y. Qin, A light sensitive nanogenerator for self-powered UV detection with two measuring ranges, Adv. Opt. Mater. 5 (1) (2017) 1600623.
[16] L. Cheng, Q. Xu, Y. Zheng, X. Jia, Y. Qin, A self-improving triboelectric nanogenerator with improved charge density and increased charge accumulation speed, Nat. Commun. 9 (1) (2018) 3773.
[17] L. Zhang, L. Cheng, S. Bai, C. Su, X. Chen, Y. Qin, Controllable fabrication of ultrafine oblique organic nanowire arrays and their application in energy harvesting, Nanoscale 7 (4) (2015) 1285–1289.
[18] A.F. Diaz, R.M. Felix-Navarro, A semi-quantitative tribo-electric series for polymeric materials: the influence of chemical structure and properties, J. Electrost. 62 (4) (2004) 277–290.
[19] A. Peigney, Ch Laurent, E. Flahaut, R.R. Bacsa, A. Rousset, Specific surface area of carbon nanotubes and bundles of carbon nanotubes, Carbon 39 (4) (2001) 507–514.
[20] F.R. Fan, L. Lin, G. Zhu, W. Wu, R. Zhang, Z.L. Wang, Transparent triboelectric nanogenerators and self-powered pressure sensors based on micropatterned plastic films, Nano Lett. 12 (6) (2012) 3109–3114.

**Mingmin Hao** received his B.E. degree in Materials Science and Engineering from Northwestern Polytechnical University (2019). He is currently a M.D. student in Lanzhou University. His research mainly focuses on self-powered gas sensor.

**Ruichao Zhang** received his B.S. in Material Physics from Lanzhou University, China in 2015. Now he is a Ph.D. student in School of Materials and Energy of Lanzhou University at Institute of Nanoscience and Nanotechnology. His research mainly focuses on energy harvesting.

**Xiaofeng Jia** received his B.S. degree in Materials Chemistry from Tianjin University of Technology (2013) and Ph.D. degree in Materials Physics and Chemistry supervised by Prof. Yong Qin from Lanzhou University (2021). He is currently a research scientist at Ji Hua Laboratory of Guangdong Province. His research mainly focuses on the preparation of low-dimensional semiconductor materials and fabrication of functional nanodevices.

**Xiang Gao** received his B.E. in Material Shaping and Control Engineering from Northeastern University, China in 2019. Now he is a M.D. student in School of Materials and Energy of Lanzhou University at Institute of Nanoscience and Nanotechnology. His research mainly focuses on Triboelectric Nanogenerator.

**Weihao Gao** received his B.S. in Material Chemistry from University of Science and Technology of China in 2016. Now he is a Ph.D. student in School of Materials and Energy of Lanzhou University at Institute of Nanoscience and Nanotechnology. His research mainly focuses on nanogenerators and functional nano devices.

**Li Cheng** received his B.S. (2011) in Physics and Ph.D. (2016) in Material Physics and Chemistry from Lanzhou University. Now he is an associate professor in School of

Materials and Energy of Lanzhou University at Institute of Nanoscience and Nanotechnology. His research mainly focuses on charge transfer and 2D materials.

**Yong Qin** received his B.S. (1999) in Material Physics and Ph.D. (2004) in Material Physics and Chemistry from Lanzhou University. From 2007–2009, he worked as a visiting scholar and Postdoc in Professor Zhong Lin Wang's group at Georgia Institute of Technology. Currently, he is a professor at the Institute of Nanoscience and Nanotechnology, Lanzhou University, where he holds a Cheung Kong Chair Professorship. His research interests include nanoenergy technology, functional nanodevice and self-powered nanosystem. Details can be found at: http://yqin.lzu.edu.cn.